Review

Check for updates

Applications of smartphone-based near-infrared (NIR) imaging, measurement, and spectroscopy technologies to point-of-care (POC) diagnostics

Wenjing HUANG[1,2*], Shenglin LUO[3,4*], Dong YANG[5*], Sheng ZHANG[1,6✉]

[1]*Ningbo Research Institute, Zhejiang University, Ningbo 315100, China*
[2]*Department of Bioengineering, School of Engineering, The University of Tokyo, Tokyo 113-8656, Japan*
[3]*Institute of Combined Injury, State Key Laboratory of Trauma, Burn and Combined Injury, College of Preventive Medicine, Third Military Medical University, Chongqing 400038, China*
[4]*Athinoula A. Martinos Center for Biomedical Imaging, Department of Radiology, Massachusetts General Hospital, Harvard Medical School, Charlestown 02129, USA*
[5]*Division of Biomedical Engineering, Renal Division, Department of Medicine, Brigham and Women's Hospital, Harvard Medical School, Cambridge 02139, USA*
[6]*State Key Laboratory of Fluid Power and Mechatronic Systems, Zhejiang University, Hangzhou 310027, China*

Abstract: The role of point-of-care (POC) diagnostics is important in public health. With the support of smartphones, POC diagnostic technologies can be greatly improved. This opportunity has arisen from not only the large number and fast spread of cell-phones across the world but also their improved imaging/diagnostic functions. As a tool, the smartphone is regarded as part of a compact, portable, and low-cost system for real-time POC, even in areas with few resources. By combining near-infrared (NIR) imaging, measurement, and spectroscopy techniques, pathogens can be detected with high sensitivity. The whole process is rapid, accurate, and low-cost, and will set the future trend for POC diagnostics. In this review, the development of smartphone-based NIR fluorescent imaging technology was described, and the quality and potential of POC applications were discussed.

Key words: Point-of-care (POC) diagnostics; Near-infrared (NIR) fluorescent imaging; Aggregation-induced emission (AIE); Smartphone-based imaging; Fluorescent probe

1 Introduction

The timeline of smartphone usage in diagnostics was included in a recent review paper (Ventola, 2014). In 2002, the Blackberry was introduced as the first mobile device with the capacity for communication and computing (Yoo, 2013). Subsequently, the first-generation iPhone (Apple) was launched in January 2007, and smartphones with the Android operating system (Google) in October 2008 (Yoo, 2013). Smartphones are readily available and their use has become pervasive across the world. According to data from the International Telecommunication Union (ITU), by the end of June 2017, the average number of mobile cellular subscriptions per 100 people was over 100 globally, 249 in Hong Kong Special Administrative Region, China, and 12 in South Sudan, Africa. In the medical field, it was reported that 87% of doctors use smartphones or tablet devices in their workplace, and 85% of medical school staff, 90% of medical residents, and 85% of medical school students use mobile devices in clinical settings at hospitals or in the classroom (Ventola, 2014). Smartphones and other mobile devices are valuable at the point-of-care (POC) because of their communication capabilities, information resources, and clinical software applications.

The opportunity to apply smartphones to the POC has resulted from not only their large number

✉ Sheng ZHANG, szhang1984@nit.zju.edu.cn

* The three authors contributed equally to this work

Sheng ZHANG, https://orcid.org/0000-0001-5599-6261

and fast spread across the world but also their improved imaging/diagnostic functions (Breslauer et al., 2009; Smith et al., 2011; Rateni et al., 2017). As a tool, the smartphone is regarded as a part of a compact, portable, and low-cost system for real-time POC, even in locations with few resources, such as a remote mountain village. With the help of the smartphone networks, community health workers at POC can share information on initial diagnostic tests and treatment with expert providers located far away. Improved functions of smartphones also promote their usage at POC. Smartphones provide various types of software applications with diverse functions including information and time management using notes, health record maintenance and access, reference and information gathering using textbooks, and even patient monitoring using collected clinical data, for use at the POC (Ventola, 2014). Recently, smartphones have been applied as an imaging modality to visualize tissues or even cells for diagnosing disease using visible light, green fluorescent proteins (GFPs), and near-infrared (NIR) light (Zhu et al., 2011b, 2012; Chung et al., 2018). This demonstrates that the usage of smartphones at the POC has entered "the deep-water area." However, no previous papers have systematically evaluated the effectiveness of smartphones in the field of diagnostics through the imaging techniques which have become possible by the incorporation of newly developed hardware such as smartphone spectrometers, or the smart usage of the original smartphone imaging tools.

In this review, we pointed out that there is a growing trend in the development of smartphone-based NIR imaging, measurement, and spectroscopy to improve the quality and applicability of POC. The techniques of NIR imaging, measurement, and spectroscopy present exciting opportunities for the following reasons.

Smartphones are widespread, even in poor areas of the world, and are an indispensable platform for the promotion of POC. As a hand-held device, the size of any associated opto-mechanical attachments should be comparable to that of the smartphone and provide advantages in manipulating test samples in microstructures (microfluidic devices). Therefore, attachments to the smartphone are always very compact, with some being only a few hundred micrometers having been fabricated as a "lab on a smartphone" using microfabrication techniques. There is one problem arising from the use of microfluidic devices: viruses are transparent compared to the many materials such as polydimethylsiloxane

(PDMS) commonly used for such devices (Männik et al., 2012; Wu et al., 2015b). Thus, it was difficult to distinguish viruses from the background because of interference between the boundaries of the microfluidic device and bacteria. In this case, phase-contrast imaging or fluorescent imaging with auto-fluorescence may not provide sufficient contrast, and the NIR spectral range provides a reliable tool for clear imaging (Männik et al., 2012; Wu et al., 2015a). The wavelength ranges of 700–900 nm (NIR-I) and 1000–1700 nm (NIR-II) have been acknowledged as biological windows for NIR fluorescence imaging (Fig. 1). Owing to the extremely low autofluorescence and absorption of water, oxygenated/deoxygenated blood, fatty tissue, and organisms, NIR can minimize background interference, and improve tissue depth penetration and image sensitivity without relying on invasive ionizing radiation (Frangioni, 2003).

A hardware system for NIR imaging may be realized by the application of fluorescent smartphones, which have been well established as a low-cost and more compact platform. The imaging quality or performance of NIR-based cell-phones will be greatly enhanced, because NIR imaging has advantages such as low auto-fluorescence (low background) and a low absorption rate (deeper tissue penetration) compared to visible light or fluorescence (Zhou et al., 2016). If probes are available, bacteria can be observed using a smartphone simply by inserting a test sample into the light path of the smartphone-based microscope system. There have been tens of such systems developed for POC diagnosis through white light or visible fluorescence. There is thought to be almost no technical barrier between the application of visible fluorescent imaging and NIR imaging. In a lab-based system, manufacturers need only to change the blue/green light-emitting diodes (LEDs) to LEDs-emitting light at the NIR spectral range. Cheap LEDs, thin-film filter membranes, externally applied lenses for magnification or light collimation, a sample holder, and so on, could be purchased from online shops, and the total cost could be only tens of US dollars.

Indocyanine green (ICG) was the first NIR fluorescent dye approved for use in the human clinical field by the US Food and Drug Administration (FDA) and European Medicines Agency (EMA) (Zhou et al., 2016). Since then, more than 17 types of NIR organic and inorganic (nanoscale) fluorophores have been
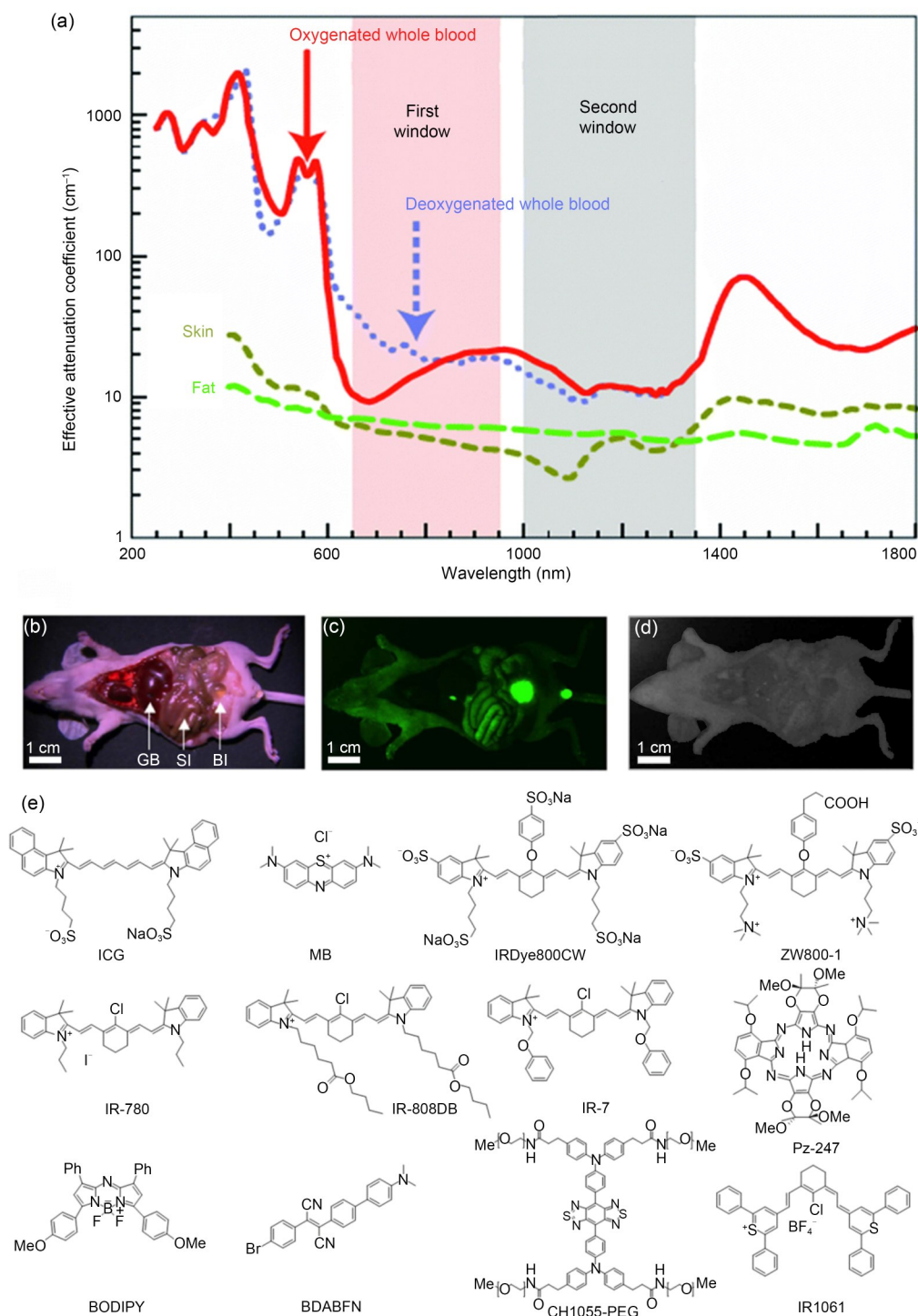
Fig. 1 Near-infrared (NIR) biological windows. (a) Absorption coefficient (on a log scale) of oxygenated blood, deoxygenated blood, fatty tissue, and water in NIR-I and NIR-II wavelengths. (b) Image of the viscera of an athymic nude mouse taken immediately after sacrifice. The arrows indicate the location of the gall bladder (GB), small intestine (SI), and bladder (Bl). Tissue autofluorescence was imaged using different excitation/emission filter sets: (c) blue/green (460−500 nm/505−560 nm) and (d) NIR (725−775 nm/790−830 nm). The results show extremely low absorption and autofluorescence of biological samples in the NIR range (Frangioni, 2003). Reprinted with permission from Frangioni (2003), copyright 2003 Elsevier. (e) Some representative organic NIR fluorophores used in clinical or preclinical applications (Luo et al., 2011). Modified and reprinted with permission from Luo et al. (2011), copyright 2011 Elsevier.

developed for preclinical or clinical research in the field of biomedical engineering using lab-based imaging systems (Hong et al., 2017). If a smartphone-based platform for NIR fluorescent imaging is established, it can be regarded as a lab on a smartphone, so there is no technical barrier to applying the well-developed NIR fluorophores for biomedical engineering on the platform. The application of NIR fluorophores to a smartphone-based platform for the observation of an extracted sample should be a non-invasive method. Therefore, the application of such a platform should greatly promote the use of different types of NIR fluorophores in specific testing fields, such as the observation of bacteria and viruses (Qi et al., 2016). Since antimicrobial resistance is increasing, more accurate methods are needed to diagnose bacterial infections and for use as tools for preclinical studies (Heuker et al., 2016). The development of a smartphone-based system with the application of NIR fluorophores should further promote research on the observation of bacteria or viruses, even at the nanoscale level (Wei et al., 2013), and eventually improve the performance of the platform as a precise diagnostic tool at the POC.

Here, we systematically describe the development flow and building blocks of smartphone-based NIR fluorescent imaging and its application to POC, from the basic techniques to the final goals (Fig. 2).

To state the flow and trends clearly, we will cover basic research such as fundamental studies on visible/NIR fluorophores, the development of smartphone systems for observation, promising techniques that will increase the usage of smartphone-based NIR imaging and establish its applicability, and applied research in the biomedical field which will eventually open the door to its widespread adoption.

2 Development of the techniques of NIR fluorescent imaging

2.1 Lab-based systems for NIR imaging

NIR imaging techniques have been used in the field of biomedical engineering with or without NIR fluorophores (Troyan et al., 2009; Chen et al., 2014; Dias, 2015; Zhu and Sevick-Muraca, 2015; Hong et al., 2017). Many kinds of commercial NIR imaging devices have emerged. In systems without NIR fluorophores, because the interaction of NIR lights with deoxyhemoglobin and oxyhemoglobin is stronger than that with water, lipids, and so on, there is also a contrast between the deoxyhemoglobin and oxyhemoglobin. NIR spectroscopy (NIRS) systems were conventionally used for the measurement of physiological parameters such as tissue oxygenation changes (Vaithianathan et al.,
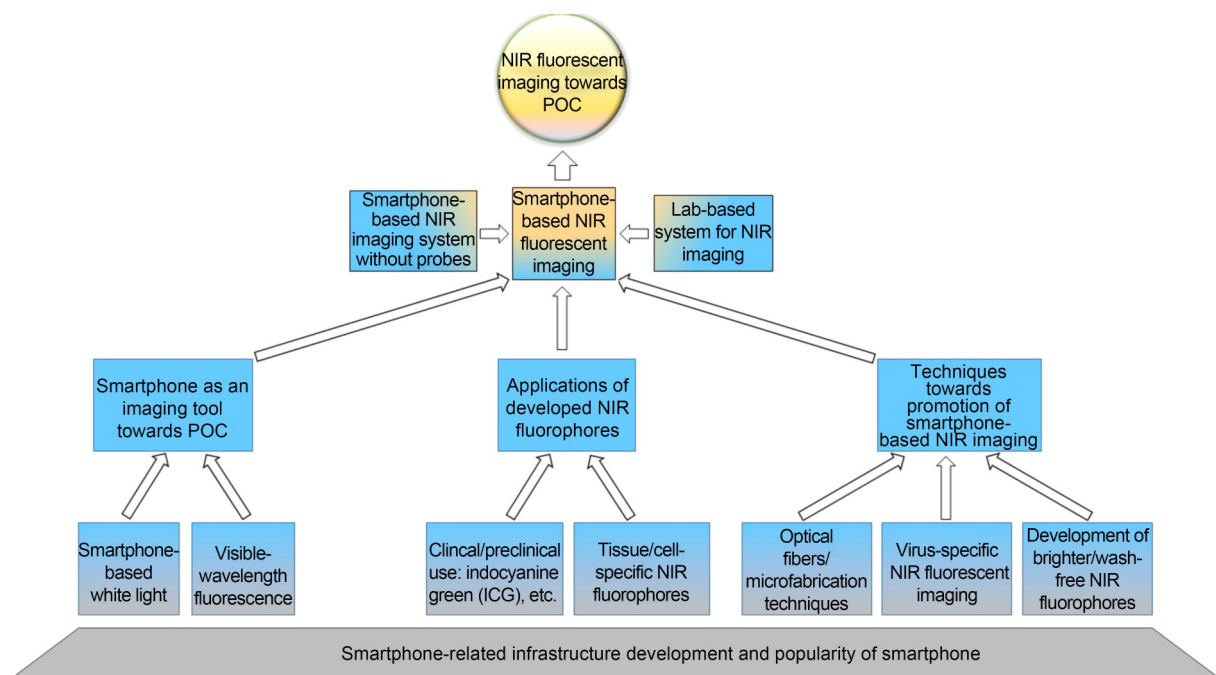

Fig. 2 Development flow and building blocks of smartphone-based near-infrared (NIR) fluorescent imaging.

2004; Kim et al., 2011). The historical background of NIRS, NIR light propagation in tissues, the basic law for measurements, kinds of NIRS systems, NIRS treatment algorithms, and NIRS instrumentation have been summarized by Dias (2015). LEDs or laser diodes (LDs) have been used extensively as light sources, and LDs may have high tissue penetration (Rolfe, 2000). For a higher contrast between hemoglobin and oxyhemoglobin, it was recommended to choose a combination of light sources with wavelength of 760 or 690 nm paired with 830 nm (Strangman et al., 2003). There are various kinds of detectors of reflections, such as the large-sized photomultiplier tube (PMT), the avalanche photodiode (APD), the silicon photodiode (SPD), and the small-sized photodiode OPT101 (Achigui et al., 2008; Zhang et al., 2009; Safaie et al., 2013).

NIR fluorescence imaging is regarded as an "emerging biomedical imaging modality" with high spatial resolution and increasing tissue penetration depths using fluorescent labels of molecular or functional reporters (Hong et al., 2017). NIR light excites the fluorescent labels within the tissues, and the generated fluorescence is imaged to determine the distribution of the imaging reagent (Zhu and Sevick-Muraca, 2015). The components of lab-based NIR fluorescence imaging devices for ICG imaging were reviewed by Zhu and Sevick-Muraca (2015). The core components include light sources for the excitation of fluorescent agents, optical filters, and detectors. There are more than ten types of devices for ICG imaging, and light sources may be LDs, LEDs, or xenon (the filtered lamp sources), with excitation wavelengths ranging from 760 to 806 nm (Zhu and Sevick-Muraca, 2015). Interference filters are used to cut out noise such as weak fluorescent signals and ambient light (Zhu et al., 2010). In previous studies, filters such as an 800-nm long-pass filter (FF01-800/LP-25, Semrock, Inc., USA) have been applied (Michael, 2010). The light incident angle is critical for maximal spectral performance and should be close to the angle of normal incidence (Michael, 2010). Collimation optics have been designed for reducing excitation light leakage (Zhu et al., 2010). Charge-coupled device (CCD) detectors are mostly used for fluorescence imaging (Zhu and Sevick-Muraca, 2015).

2.2 Development of NIR fluorophores for lab/clinical use

The developed NIR fluorophores include cyanine dyes, porphyrin derivatives, phthalocyanines, squaraine, and boron dipyrromethane analogues, as reviewed by Luo et al. (2011). The FDA approved the first NIR fluorophore, ICG, for clinical use more than half a century ago (Fig. 1e), followed by methylene blue (MB; emission about 700 nm). ICG binds to cell plasma protein and has absorption and emission peaks of around 807 and 822 nm, respectively (Schaafsma et al., 2011). IRDye800CW has been approved for NIR imaging in clinical trials. Luo et al. (2011) introduced a cyclohexenyl substitution and two amphipathic *N*-alkyl side chains into ICG. The modified NIR fluorophore can be used not only for NIR imaging but also for targeting cancer-cell mitochondria, chemotherapy, photodynamic therapy (PDT), and photo-thermal therapy (PTT) (IR-780, IR-808DB, IR-7) (Tan et al., 2017). Similar to cyanine dye IR-780, another NIR dye Pz-247 from porphyrin derivatives has also been identified with tumor-preferential accumulation, which is very useful for cancer-selective detection and early diagnosis (McAuliffe et al., 2017). Tang et al. (2015) reported a series of interesting NIR probes with the novel property of aggregation-induced emission (AIE) (Ding et al., 2013). They emit NIR fluorescence only when aggregated (e. g., molecule 2-(4-bromophenyl)-3-(4'-(dimethylamino)-biphenyl-4-yl) fumaronitrile (BDABFN)). Hong et al. (2017) presented a list of fluorophores, including 17 common fluorescent reagents for NIR-I and NIR-II. As mentioned before, NIR-I refers to the traditional NIR window (700–900 nm), and NIR-II is the NIR window ranging from 1000 to 1700 nm (Zhao et al., 2018). CH1055-PEG and IR1061 are examples of NIR-II fluorophores. Apart from small organic molecules, different kinds of elaborate inorganic nanomaterials were also used as NIR fluorophores, such as quantum dots (QDs), single-walled carbon nanotubes, and rare-earth nanoparticles. Both organic and inorganic fluorophores have been applied to target specific tissues such as cartilage or bone, liver, and tumors (Shu et al., 2009; Pansare et al., 2012; Hyun et al., 2014, 2015; Antaris et al., 2016; Shcherbakova et al., 2016).

The use of tissue-specific fluorophores is regarded as a key technique to distinguish diseased from vital tissues (Chen et al., 2008; Neuman et al., 2015). Owens et al. (2016) discussed the principle of the use of two distinct imaging channels of NIR light from 650 to 900 nm to achieve tissue-specific fluorescent imaging. Optical filters can be applied to detect two NIR wavelengths (700 nm for normal, and 800 nm for diseased

tissues) excited by light sources or visible light separately or simultaneously. Based on these considerations, various methods have been proposed to achieve tissue-specific NIR imaging. For example, the vasculature may be leaky in tumor tissues but non-permeable in normal tissues, and a contrast agent can enter the tumor tissue selectively (Owens et al., 2016). Specific expression of surface biomarkers of cancer cells is also applicable for selectively imaging tumor tissues, as these markers have been investigated extensively (Dinjaski et al., 2014; Tang et al., 2015). A method called "activatable targeting" has also been considered (Owens et al., 2016). The fluorescence of the NIR fluorophore is quenched using methods such as pH-sensitive moieties when the agents pass through the body, and becomes activated by specific microenvironmental factors such as pH, only after arrival in the diseased tissues (Urano et al., 2008).

The recombination of NIR fluorescent proteins with viruses has been tested for tumor targeting. Sakuda et al. (2019) developed a bioimaging system by combining the vesicular stomatitis virus (VSV) with an NIR fluorescent protein called Katushka, to form the recombinant VSV-Katushka. VSV is bound to osteosarcoma cells specifically because tumor cells do not have the antiviral interferon signaling pathways (Sakuda et al., 2019). Using the osteosarcoma cell-specific agent, the tumor margins were demonstrated as a fluorescent area for resection (Sakuda et al., 2019).

3 Smartphones as an imaging tool for POC: from white light to fluorescence

As an interface device, smartphones have been used as platforms to control portable diagnostic systems such as NIRS systems (Watanabe et al., 2016). In such systems, the smartphone is connected to a system containing three built-in NIR LEDs and a single silicon p-type/intrinsic/n-type (PIN) photodiode. The system (PocketNIRS Duo and PocketNIRS HM) was used as a monitor for brain and arm muscle hemodynamics and oxygenation based on the modified Beer-Lambert law (Watanabe et al., 2016). The smartphone is a promising diagnostic tool at POC based on the abovementioned advantages. In contrast to systems using the smartphone in a control function, other techniques have been developed for the efficient use of smartphone cameras. Smartphones equipped with complementary metal oxide semiconductor (CMOS)

detectors can collect images using either visible or NIR light (Ghassemi et al., 2017).

Imaging using white-light is the most basic imaging modality of a smartphone-based microscope system. It is generally used together with a combination of blue, green, or red color imaging. The mobile phone is opto-mechanically attached to the microscopy system. For bright-field imaging, a cheap microscope eyepiece, an objective, and a white LED for illumination are necessary. A field-of-view of about 180-μm diameter with a spatial resolution of about 1.2 μm was realized using a 0.85 numerical aperture (NA) 60× Achromat objective and a 20× eyepiece (Breslauer et al., 2009).

Smartphone-based imaging techniques based on visible light may afford lessons for the development of the device for NIR fluorescent imaging. Applications of the cameras involved in white-light, GFP, and NIR light were discussed below.

3.1 Smartphone-based imaging using visible-wavelength fluorescence

Smartphone-based fluorescent imaging of cells, viruses, and molecules has been realized using a combination of external and built-in lenses. Normally, LEDs or LDs are added to the white LEDs, and filter membranes are used to cut out noise or for a dark field. Using a three-dimensional (3D) printing technique, Kühnemund et al. (2017) established a system which is lightweight and capable of being attached opto-mechanically to a mobile phone. To obtain fluorescence and bright-field images, the optical attachment is equipped with laser diodes at 532 and 638 nm, and a white LED. The sample holder consists of motorized stages for *x*-, *y*-, and *z*-movement for focus adjustment (Kühnemund et al., 2017).

Zhu et al. (2012) developed a method to detect *Escherichia coli* using a smartphone. A filter and an external lens were placed between the sample and the built-in lens of the smartphone. *E. coli* in contaminated water and food was captured by anti-*E. coli* O157:H7 antibodies immobilized onto a capillary tube with an inner diameter of about 100 μm, and streptavidin-conjugated QDs with fluorescence emission were introduced as a fluorescent reporter. Ultra-violet (UV) LEDs were butt-coupled to the capillary tube, and the liquid sample in the tube acted as a light waveguide along the tube. Because the light is perpendicular to the detection path, an inexpensive long-pass glass filter can be used to remove the scattered light and obtain a dark-field background (Zhu et al., 2012).

Wide-field fluorescent imaging (about 81 mm^2) on a Sony-Erickson U10i Aino smartphone with a spatial resolution of about 20 μm was also established by Zhu et al. (2011a, 2011b). Imaging of a large sample area and volume can be realized using such a system. In this system, the excitation light is also perpendicular to the detection path, and therefore, an absorption filter is sufficient for the creation of a dark-field background. To achieve wide field, they placed a lens directly above the built-in smartphone lens to create a de-magnification of 3.2 for imaging of the fluorescent samples (Zhu et al., 2011c).

Zhu et al. (2011a) developed fluorescent imaging cytometry for bodily fluids and water samples on a Sony-Erickson U10i Aino smartphone. The optofluidic attachment consists of a flat microfluid chip, LEDs directly butt-coupled to the chip, an absorption filter, and an external lens for magnification located right above the built-in lens of the smartphone. Fluorescently labeled samples were injected into the microfluid chip by an external syringe pump. Videos of the labeled cells/particles were obtained at a frame rate of about 7 fps (frames per second), and the number of targets was counted through the videos. Based on the principle of optofluidic wave-guiding, the excitation light is confined inside the microchannel, and a simple plastic absorption filter can be used to cut out the scattered pump photons because the fluorescent light is perpendicular to the detection path (Zhu et al., 2011b). Infection with human cytomegaloviruses (HCMV), which range from 150 to 300 nm in diameter, may lead to virus-associated birth defects (Huang and Johnson, 2000; Haspot et al., 2012). To detect single nanoparticles or viruses using a smartphone-based microscope, Wei et al. (2013) applied a high-power laser diode (75 mW) with an excitation center at 450 nm to strengthen the fluorescence arising from nanoparticles (sizes ranging from 10 μm to 100 nm) or labeled HCMV. The incidence angle of the excitation light was 75°. A long-pass filter was used to cut out the scattered excitation light. Focus adjustment was realized by the application of a miniature dovetail stage (DT12, Thorlabs). Fluorescent images with 2× magnification were obtained by using a combination of the external lens and the lens of the smartphone (Wei et al., 2013).

3.2 Smartphone-based diagnosis using NIR spectral analysis

Many smartphone-based diagnoses using NIR light are now emerging (Fig. 3). There is even a miniaturized NIR grating spectrometer developed specifically as a light source for smartphone applications at Fraunhofer intelligent pain management system (IPMS), covering wavelengths from 950 to 1900 nm (Fig. 3a) (Pügner et al., 2016). A smartphone-based system with an NIR illuminant has been used in pulse oximetry to monitor blood oxygenation levels (Kanva et al., 2014; Scott et al., 2014; Bui et al., 2017; Holz and Ofek, 2018; Vanegas et al., 2018). Haemoglobin is an important component of blood. Oxygen binds with haemoglobin to form oxy-haemoglobin, making it soluble in blood. To measure oxygenation levels, smartphone camera oximetry must be capable of distinguishing reflections from oxyhaemoglobin and deoxyhemoglobin. NIR illuminants based on Beer-Lambert law typically are used to detect reflections from deoxyhemoglobin (Chance et al., 1988; Kim and Liu, 2007).

Hussain et al. (2018) designed an optical device attached to a Sony Xperia E3 smartphone (Android 4.4.3 lollipop) for the detection of light from the visible to near infra-red spectroscopic regions (Fig. 3b). The ambient light sensor of the smartphone was used to sense the spectra in the range of 350–1000 nm, instead of applying the smartphone CMOS camera. The optical system contains two types of LEDs as light sources, with peak emission wavelengths of 510 and 880 nm, respectively. Light filters were not used because the cost is higher than that of LEDs with a specific wavelength. The two external LEDs were chosen based on the results of spectrophotometric analysis of the two samples, iron (II) and phosphate solutions, using a standard laboratory-grade spectrophotometer (UV-3600 Plus UV-Vis-NIR Spectrophotometer, Shimadzu, Japan). The LEDs were powered by the internal battery of the smartphone through a USB-OTG cable. The LED light beam was collimated by an external collimating lens and propagated through the sample solution. The ambient light sensor then detected the intensity of the transmitted light beam via a focusing lens, and the sample concentration was measured based on the Beer-Lambert law of absorption. Using this smartphone-based optical system, samples with various concentrations were measured correctly according to device calibration by Hussain et al. (2018). There are also commercially available smartphones for food scanning, in which an NIR camera or spectrometer has been installed (Fig. 3c). Liang et al. (2014) used a smartphone to detect microbial spoilage on ground beef under an 880-nm NIR LED. The specific scatter signals at various angles were associated with the *E. coli* concentration on the meat (Fig. 3d).

Antibodies were not applied in the study. Instead, Mie scattering was used as a parameter to demonstrate the bacterial concentration. *E. coli* tends to bind to fat cells. The averaged refractive index of pure lipids is 1.460 and the refractive index of the bacteria is 1.388. Both indexes are higher than that of water (1.327). Although the difference is small, pure lipids could be distinguished from the flat surface with the colonies of *E. coli*. Mie scattering is dependent on the angles of scatter detection and bacterial concentrations. Long et al. (2017) established the system based on these principles. The LED was irradiated perpendicular to the meat surface and the camera of an iPhone 4S detected the signal angled at 15°–60° from the incident light at different bacterial concentrations. Kaile and Godavarty (2019) developed an NIR smartphone-based imaging system to measure in vivo the hemoglobin-related oxygenation changes beneath the surface of the skin (Fig. 3e).

3.3 Smartphone-based NIR fluorescent imaging

Compared to systems without the use of NIR fluorophores, smartphone-based fluorescence microscope systems are an emerging technology. Currently, only a small number of groups are conducting research in this field. The CMOS detector of a smartphone is said to be sensitive to light in the visible and NIR regions, but manufacturers usually use a short-pass filter to cut off NIR wavelengths (Ghassemi et al., 2017). Ghassemi et al. (2017) removed the short-pass filter and evaluated the effectiveness of a smartphone-based system using NIR fluorescence imaging (Fig. 4a). The external part of the system contained an LED (M780L3, Thorlabs, Inc., Newton, NJ, USA) with a 780-nm center wavelength as an external light source, an 800-nm short-pass filter (84-729, Edmund Optics, Barrington, NJ, USA) as an excitation filter, and a convex lens and diffuser to obtain uniform illumination. A long-pass emission filter was attached to the smartphone camera following the removal of the NIR blocking filter. ICG (Pulsion Medical Inc., Powell, OH, USA) was used as the primary fluorophore. It was injected into the channels of a 3D-printed tissue phantom or a Lewis rat model to determine the spectral sensitivity of the smartphone camera in the range of 700–1100 nm. The quality of smartphone-based NIR
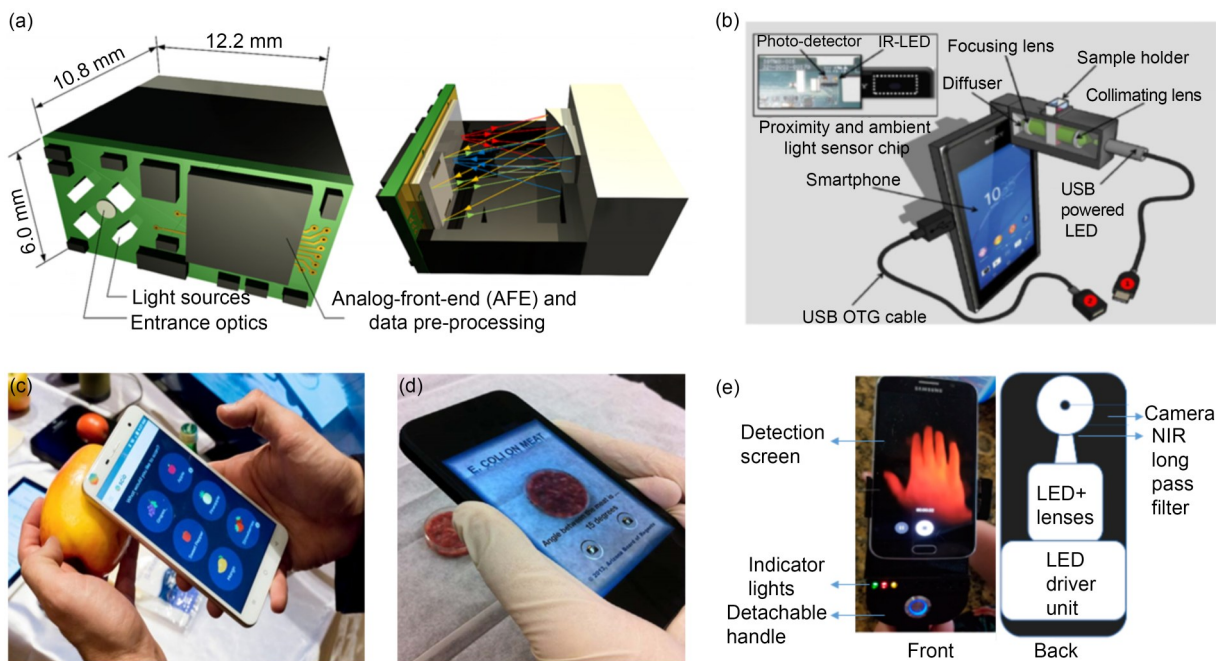

Fig. 3 Smartphone-based near-infrared (NIR) fluorescent imaging devices without NIR fluorophores. (a) Rendered image of a cell-phone-based NIR spectrometer and a sectional view of the same system with the optical path (red, orange, green, and blue) highlighted (Pügner et al., 2016); (b) A compact design of an NIR spectrometer on a cell-phone (Hussain et al., 2018); (c) Smartphone-based NIR spectrometer for food detection (SCiO, Consumer Physics, Israel); (d) A smartphone developed for detecting microbial spoilage on ground beef under an 880 nm NIR LED (Liang et al., 2014); (e) An NIR smartphone-based imaging system developed to measure hemoglobin-related oxygenation changes beneath the surface of the skin (in vivo) (Kaile and Godavarty, 2019) (Note: for interpretation of the references to color in this figure legend, the reader is referred to the web version of this article).

fluorescence imaging was almost as good as that of a scientific CCD in the 3D-printed tissue phantom or the ICG-filled rodent femoral vasculature (Figs. 4b and 4c, a femoral artery bifurcation) (Ghassemi et al., 2017). This may have been the first experiment involving removal of the built-in filter of a smartphone. The study demonstrated that it is effective for NIR fluorescent imaging of the 3D-printed phantom and the ex vivo animal model. However, it is unclear whether the method and its application to in vivo imaging represent a strong trend in smartphone-based imaging as a POC task. Conservatively, it may be used only in a few high-end devices.

Chen et al. (2014) recently compared the fluorescence imaging capabilities of NIR-enabled mobile phones with or without CCD, using phantom-based test methods, and found certain aspects of performance comparable to a scientific-grade CCD (Figs. 4d and 4e). They also verified the in vivo fluorescence imaging and tumor visualization capabilities of mobile phones (Fig. 4f). Cost-effective, compact, and portable NIR mobile phones capable of wireless data transfer will inevitably fuel up the application of NIR imaging technologies in our daily life and healthcare systems (Suresh et al., 2018).

Typical elements of lab-based and smartphone-based NIR fluorescent imaging are listed in Table 1. Components of smartphone-based fluorescent imaging are shown in Table 2.

4 Techniques for further promotion of smartphone-based measurement and spectroscopy

4.1 Optical fibers for smartphone-based spectral analysis

Long et al. (2017) have developed an instrument, which used the rear-facing camera of a smartphone for investigations based on three biosensing modalities:
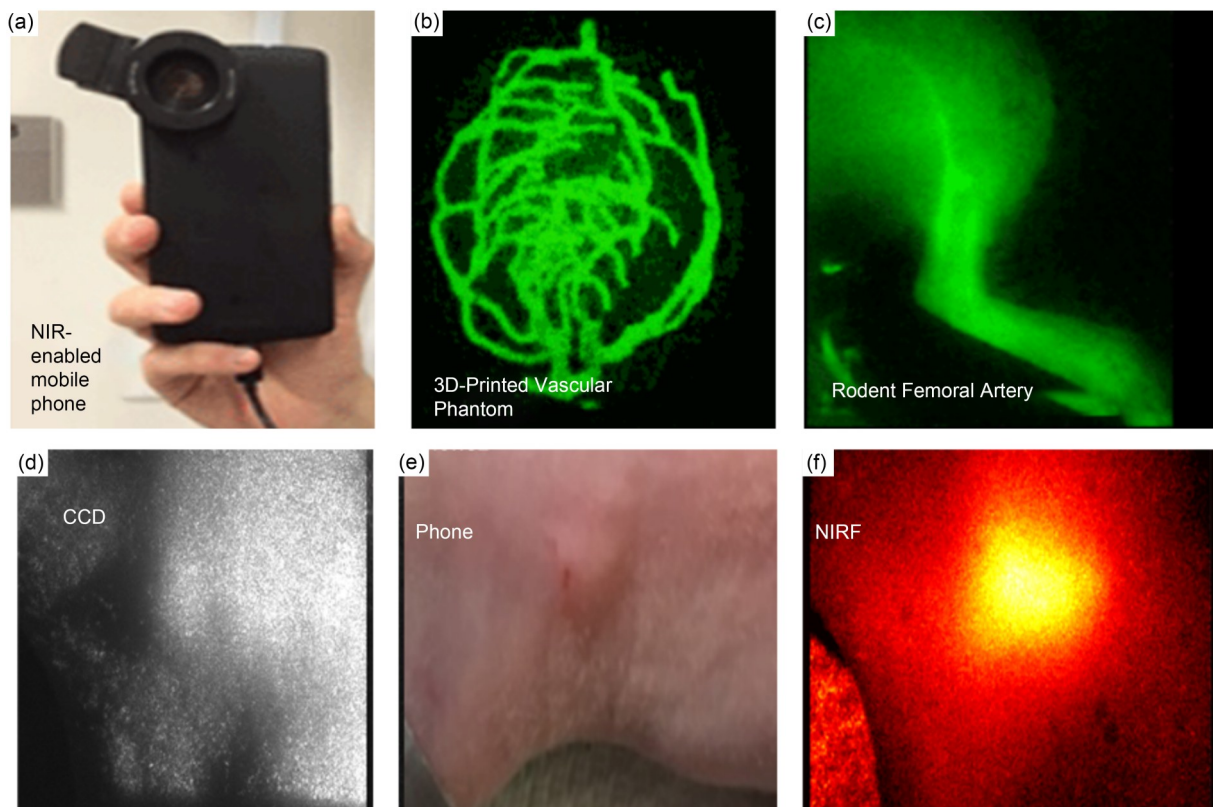

Fig. 4 Smartphone-based near-infrared (NIR) fluorescent imaging devices with NIR fluorophores. A smart cell-phone (a) installed with an NIR camera was used to image molded and 3D-printed tissue phantoms (b), and an ex vivo animal model (c). Indocyanine green (ICG) was used as an NIR probe (Ghassemi et al., 2017); white light (d, e) and in vivo fluorescence (f) imaging of a tumor by NIR-enabled mobile phones. An NIR fluorophore monoclonal antibody (mAb)-700 was synthesized by conjugating an mAb with an NIR phthalocyanine dye (IR-700), and intravenously injected into a rodent (Suresh et al., 2018).

Table 1 Typical elements of devices available for NIR fluorescent imaging

Element	Lab-based		Smartphone-based	
	Representative item	Reference	Representative item	Reference
Light source	Laser light source	Zhu and Sevick-Muraca, 2015	LED (wavelength=780 nm)	Ghassemi et al., 2017; Wang et al., 2017
	LED	Zhu and Sevick-Muraca, 2015	MEMS-based NIR grating (wavelength=950–1900 nm)	Pügner et al., 2016
	Xenon	Zhu and Sevick-Muraca, 2015		
Optical filter for image collection	Bandpass filter	Marshall et al., 2010; Sevick-Muraca et al., 2008; Troyan et al., 2009	Short-pass excitation filter	Ghassemi et al., 2017
	Notch filter	Marshall et al., 2010; Sevick-Muraca et al., 2008	Long-pass emission filter	Ghassemi et al., 2017
	Cut-on filter	Handa et al., 2009; Marshall et al., 2010		
Detector for fluorescent signals	CCD	Zhu and Sevick-Muraca, 2015	8-bit CMOS sensor (NIR blocking filter removal)	Ghassemi et al., 2017
	Electron-multiplying CCD	Zhu and Sevick-Muraca, 2015		
	Intensified CCD	Zhu and Sevick-Muraca, 2015		

NIR: near-infrared; LED: light-emitting diode; CCD: charge-coupled device; CMOS: complementary metal oxide semiconductor; MEMS: micro-electro-mechanical system.

Table 2 Typical smartphone devices used for fluorescent (visible and NIR) imaging

System	Source type/emission wavelength	Sampling/preparation	Visible fluorescence	NIR	Reference
Sony-Erickson U10i Aino™; Kodak Wratten Color Filter 12 for dark-field	Blue and white LED (Digikey Corp.)	Fluorescent bead or stained white blood cell/*Giardia lamblia*	Yes	No	Zhu et al., 2011a
Sony-Ericsson U10i Aino™; glass capillaries (inner diameter about 100 μm); long-pass glass filter for waveguide	UV LEDs	Fluorescent QD labeled *Escherichia coli* on the capillary surface	Yes	No	Zhu et al., 2012
Nokia smartphone PureView 808; long-pass filter FF01-500/LP-23.3-D, Semrock	Blue LD centered at 450 nm (75° incidence angle)	Green fluorescent polystyrene particle of 100 nm; fluorescently labeled human cytomegaloviruses	Yes	No	Wei et al., 2013
Nokia Lumia 1020 smartphone; external lens; dual-band emission filter	A white LED; LDs 532 nm at 75 mW and 638 nm at 180 mW, Mitsubishi Electric (about 75° incidence angle)	Micron-sized DNA coils inside preserved cells and tissues	Yes	No	Kühnemund et al., 2017
Smartphone (no brand information); external lens; excitation filter; emission filter; *Z*-stage	8 LEDs	Fluorescently labeled *Giardia* cysts	Yes	No	Koydemir et al., 2015
Smartphone (no brand information); short-pass excitation filter; long-pass emission filter; zoom lens; convex lens; diffuser	LED with 780 nm center wavelength	3D-printed phantoms; ex vivo rodent model	No	Yes	Ghassemi et al., 2017

NIR: near-infrared; LED: light-emitting diode; UV: ultra-violet; LD: laser diode; 3D: three-dimensional; QD: quantum dot.

light transmission for in vitro diagnostic (IVD) tests such as enzyme-linked immunosorbent assay (ELISA) assays, reflectance spectroscopy for IVD tests such as surface plasmon resonance (SPR) biosensing, and intensity spectroscopy for IVD tests such as fluorescence or chemiluminescent immunoassays (far-infrared ray (FIR), chemiluminescent immunoassay (CLIA)). Optical fibers, a photonic crystal biosensor (reflection mirror), lenses, and a green LED were assembled into a 3D-printed cradle (FormLabs Form 2 at a resolution

of 50 µm) with precise optical alignment. One optical fiber was used to collect white light from the light source (the rear flash LED of a smartphone) for the transmission and reflectance modalities. For the intensity modality, the flash LED of the smartphone was turned off and a 532-nm laser diode (green light) was turned on. A collection lens was used to focus the light within the test sample for maximal fluorescence collection. After the light passed through the test sample, the other optical fiber was used to direct the light to the rear camera of the smartphone. In the study, the test samples were introduced to the light path using a microfluidic cartridge, and samples could be manipulated using an eight-channel multi-pipette (Long et al., 2017).

4.2 Cell separation/sorting techniques

To apply a smartphone-based system to NIR imaging, measurement, and spectroscopy at POC, there must be sophisticated supporting techniques such as methods for specific cell capture and cell sorting. Knowlton et al. (2017) developed a device capable of first separating cells based on magnetophoresis-based cytometry, and then imaging them. Cells can be separated according to their density in a paramagnetic medium using the method of magnetic focusing: cells are levitated at a height in the medium due to the resultant force of magnetic and buoyant forces. The buoyant forces are determined by the density of the cells relative to the density of the medium (Mirica et al., 2009; Nemiroski et al., 2016; Knowlton et al., 2017). A 3D-printed microscopy system (FormLabs Form 1 at a resolution of 0.1 mm), containing a phone case, optical components, and emission filter holders, was applied. A Samsung Galaxy S6 was used because it offers manual focusing. Two nickel-plated neodymium-iron-boron (NdFeB) permanent magnets aligned along the longitudinal direction of the rear face of the smartphone and a glass capillary tube with the test sample were located between the two magnets. A gadolinium-based medium, Gadavist (Bayer, Whippany, NJ, USA), was used as a paramagnetic agent, and only cells levitating at the desired height, not those at the bottom of the microcapillary or at a different height, were visible. Using this method, rare diseased cells could be separated from healthy cells within a large population. For example, ovarian cancer cells HeyA8 were distinguished from cells in diluted blood, because the two cell types had different densities and therefore were spatially separated

at different heights with respect to the microscope focus in the magnetic field (Knowlton et al., 2017). Koydemir et al. (2015) developed a smartphone-based fluorescent microscopy technique with a capturing method for the detection of cysts of the most common waterborne parasite, *Giardia lamblia* (Ceylan Koydemir and Ozcan, 2018). The waterborne transmission of parasitic protozoa can lead to outbreaks of human diseases (Baldursson and Karanis, 2011). Using porous filter membranes with a 5-µm pore size for capturing the cysts, Koydemir et al. (2015) designed a sample holder within the microscopy system to separate these bacteria from water samples of about 20 mL. Diluted stain (200 µL) was added to a water sample before the separation process. A Nokia Lumia 1020 smartphone was used (Wei et al., 2013, 2014), and eight blue LEDs provided the external light source for even light distribution. A large field of view (FOV) of about 0.8 cm^2 was achievable.

4.3 Microfabrication techniques

Pügner et al. (2016) developed an NIR grating spectrometer (micro-electro-mechanical system (MEMS) devices) for smartphone applications using sophisticated microfabrication techniques with lithography (Fig. 3a). For applications in a mobile phone, the spectrometer should have a spectral range from 950 to 1900 nm with a resolution equal to or less than 10 µm. One nanometer is necessary for long-term wavelength stability. Further, the absorbance (*A*) value should be from 3.5 to 4.0 to ensure that the absorption measurements are suitable for smartphone analysis according to the Beer-Lambert law. As an inbuilt part of a smartphone, the device size should be smaller than 20 mm×20 mm×6 mm (thickness). A Czerny-Turner design was applied. The principle is as follows. A curved mirror is used to collimate the light passing through an entrance slit, and a rotatable grating is applied to diffract the collimated light. A second curved mirror is used to re-focus the diffracted light at an exit slit. Only light with a specific wavelength determined by the grating rotation angle can pass through the exit slit: lights with different wavelengths are eliminated because they are re-focused to a position other than the exit slit. MEMS devices were applied with a precisely defined layout. The entrance and exit slits were added to the MEMS chip. The two slits were located at defined positions with respect to a rotatable grating, taking into consideration the angles of incidence and diffraction. A resonant electrostatic-comb

drive was used to actuate the MEMS devices (Pügner et al., 2016).

5 Promising fields of application towards POC and issues to be resolved

5.1 A potential application field: smartphone-based virus or bacteria detection

Smartphone-based detection of bacteria is regarded as a state-of-the-art method (Gopinath et al., 2014). Lab-based methods have been developed to provide noninvasive visualization of virus infection in vivo, and NIR fluorescent imaging is effective for monitoring bacterial infections (Foster et al., 2008; Dinjaski et al., 2014; Pan et al., 2014). Here, NIR fluorophores used for virus imaging and related results are reviewed to evaluate the possible application of NIR fluorescent imaging to smartphone-based bacterial detection, although previous studies usually used the fluorophores for in vivo detection.

Pan et al. (2014) labeled avian influenza H5N1 pseudotype virus (H5N1p) with NIR-emitting QDs to observe the distribution of this virus in the lungs of mice. Isomura et al. (2017) have demonstrated that a recombinant rabies virus (RABV) expressing an NIR fluorescent protein iRFP720 (infra-red fluorescent protein 720) was suitable for NIR fluorescent imaging of RABV infection in nude mice. To monitor three bacterial species in the gastrointestinal tract (bacterial infection) in mice, Berlec et al. (2015) constructed *Lactococcus lactis*, *Lactobacillus plantarum*, and *E. coli* expressing the NIR fluorescent protein iRFP713 (Kleerebezem et al., 1997). The expression of iRFP713 in *L. lactis* and *L. plantarum* was constructed using the nisin-controlled gene expression (NICE) system. Take the construction of NIR fluorescent *L. lactis* as an example. The plasmid pNZ-iRFP713 in *L. lactis* NZ9000 (a host strain) contains copies of *nisRK* genes and enables binding of nisin (a 34-amino acid anti-microbial peptide). During the construction process, the nisA promoter (PnisA) (a promoter in the nisin gene cluster) on a plasmid was used to control the expression of the downstream gene (*iRFP713*) (Mierau and Kleerebezem, 2005; Zhou et al., 2006; Berlec et al., 2015). A biliverdin assay developed by Berlec et al. (2015) was used to construct the NIR fluorescent *E. coli*. A CP25 promoter in pGEM::CP25-iRFP713 plasmid, which was applied to control the transfection of iRFP713 (Berlec and Štrukelj, 2014; Berlec et al., 2015). As discussed above, NIR fluorophores have been used for the tracing of bacteria or viruses in vivo. However, a few studies have involved the application of smartphone-based NIR fluorescent imaging for bacteria or virus detection. The development of these types of fluorophores and investigation of the movement of viruses in vivo have been confirmed to be helpful in the elucidation of pathology. However, this may not have actual utility in smartphone-based NIR fluorescent imaging, which is used to survey extracted samples in the sample tray inserted into the compact microscope system (Gopinath et al., 2014). Probes available for bacteria or virus imaging are listed in Table 3.

5.2 Development of fluorophores for virus-specific NIR fluorescent imaging

Some species of bacteria are harmful to human health, but some bacteria (or bacteria in the proper amount) are necessary for the normal physiological functions of human beings (Zhao et al., 2015b). NIR probes that cannot specifically bind to one kind of bacteria may have no practical value for bacteria or virus detection in the field of POC. No NIR fluorophores have been developed for specific species of viruses. However, fluorescent imaging of a specific type of virus is possible according to a previous study, and this should become a trend for the testing of NIR fluorophores. Zhao et al. (2015a, 2015b) developed AIE luminogen (AIEgen) 4 for the evaluation of bacterial susceptibility and antibiotics screening. Only after the formation of micelles at high concentrations was fluorescence turned on. In other words, fluorescence of probes at low concentrations was not observed. Based on this phenomenon, different bacteria may be distinguished. For example, after the addition of the antibiotic kanamycin sulfate (KANA), the growth of *E. coli* was inhibited, but KANA-resistant *E. coli* still grew extensively. As a result, strong fluorescence of KANA-resistant *E. coli* but low fluorescence of *E. coli* was obtained (Zhao et al., 2015b). Therefore, such an AIEgen could be used to distinguish the two types of bacteria.

5.3 A potential application field: smartphone-based virus or bacteria detection

NIR fluorophores have proved to afford an attractive spectral choice for bacterial imaging. To provide guidelines for the engineering of fluorescent fusions in bacteria, Wu et al. (2015a) studied the combination

Table 3 Probes used in previous studies for NIR fluorescent imaging of bacteria or viruses

Type of bacteria/virus	Probe	Excitation wavelength (nm)	Emission wavelength (nm)	Condition for use	Reference
Lactococcus lactis, *Lactobacillus plantarum*, and *Escherichia coli*	iRFP713	690	713	Stomach and small intestine in live mice	Berlec et al., 2015
Bacterial peptidoglycan of *Mycobacterium smegmatis*, *Corynebacterium glutamicum*, and *Listeria monocytogenes*	NIR fluorogenic azide probe based on Si-rhodamines	655	668	No washing was necessary for staining	Shieh et al., 2014
E. coli	eqFP670	605	670	Multi-color imaging using blue, orange, and NIR probes	Wu et al., 2015a
Avian influenza A virus (H5N1p)	NIR-emitting QDs		750	Nuance FX multispectral imaging system (PerkinElmer)	Pan et al., 2014
VSV	Katsushka NIR fluorescent protein (recombinant VSV-K)	588	635	Evaluation by fluorescence microscopy (BZ-9000 microscope, Keyence)	Sakuda et al., 2019

NIR: near-infrared; VSV: vesicular stomatitis virus; QDs: quantum dots; iRFP: infra-red fluorescent protein.

of NIR fluorescent proteins with blue and orange fluorescent proteins for the observation of the nucleoid and division proteins of bacteria in vitro, respectively. The nucleoid proteins of *E. coli*, HU and *Lac*I, and the cell division proteins, *Min*D and *Fts*Z, were fluorescently labeled to test brightness and photo-stability, respectively. An NIR protein, eqFP670 (excitation/emission wavelength: 605 nm/670 nm), was used for *E. coli* imaging, because eqFP670 was said to be the most red-shifted protein and has high photo-stability (Shcherbo et al., 2010). As a result, eqFP670 is highly applicable to multi-color imaging, because it shows high brightness and photo-stability for the NIR spectral range with little cell photo-damage (Wu et al., 2015a). Wu et al. (2015a), therefore, pointed out that NIR fluorescent proteins such as eqFP670 could be used as a third or fourth color other than blue or orange, etc. for the observation of bacteria inside microstructures or microfluidic devices such as PDMS devices (Wang et al., 2010; Hol and Dekker, 2014).

5.4 Development of wash-free NIR fluorophores

A common strategy for a target probe is to conjugate a probe to antibodies that are specific for a targeted analyte or biomarker of pathogens. However, the non-specific attachment or unbinding free probe would also cause a high background noise signal and decrease detection sensitivity. To avoid this, it is necessary to wash the samples before fluorescence imaging.

The washing process is always necessary during the process of cell transfection, which increases the experimental procedures. Further, the washing process may lead to the loss of bacteria and thus decrease the accuracy of quantification analysis (Zhao et al., 2015b). Some probes for fluorescent imaging with a visible wavelength developed using the strategy of AIE emit faintly when they are dissolved in water, but the fluorescence becomes strong when the probes are aggregated (Luo et al., 2001; Mei et al., 2015). Therefore, the washing step is not necessary. Shieh et al. (2014) developed a wash-free NIR fluorogenic azide probe based on biorthogonal chemistry (Sletten and Bertozzi, 2009), and a new class of cyclooctyne-functionalized D-amino acids was incorporated into the probe (emission 670 nm) for the observation of peptidoglycan of the bacteria *Mycobacterium smegmatis*, *Corynebacterium glutamicum*, and *Listeria monocytogenes*. The development of NIR fluorogenic probes with emission wavelengths above 700 nm was thought to be challenging. The trigger for successful development was that Xiao's group found that emission in the NIR region could be achieved by replacing the oxygen atom in the xanthene moiety of tetramethylrhodamine with Si-rhodamine (Fu et al., 2008; Koide et al., 2011). Shieh et al. (2014) identified azide-functionalized Si-rhodamines that enhanced fluorescence quantum yield upon triazole formation using computational methods. The probe bound specifically to the terminal alkynes on the

mammalian cell surface. Washing of the free probes after transfection was not necessary, because the excess probes did not fluoresce during nonspecific binding events (Lukinavičius et al., 2013).

6 Conclusions

A smartphone-based microscope/imaging system has been developed as a platform for diagnosis at POC. Sooner or later, it is only natural that the techniques of NIR fluorescent imaging will be combined with smartphone technologies to afford rapid, accurate, and low-cost services related to telemedicine. In this paper, we analyzed several aspects of these trends. As a popular hand-held platform available on almost any occasion in daily life in developed and developing countries, smartphones draw a lot of attention, and the convenience they provide promotes their widespread use in research involving imaging and diagnostic techniques. Smartphone-based platforms have been developed for imaging cells, bacteria, and viruses through white light and/or fluorescence. Smartphone systems have also been used in NIR imaging to investigate the oxygenation levels in tissues. The establishment of smartphone-based microscope systems has benefited greatly from the design concepts of lab-based systems and their components such as LED light sources, light filters, collimation optics, magnifying lenses, sample trays, and *XYZ* stages. Researchers have paid attention to the layout due to the compact size of the smartphone, and the necessity of convenience for use at POC. For example, the introduction of cell capturing or sorting equipment. The development of smartphone-based

imaging systems for POC provides a robust platform for the incorporation of NIR fluorescent imaging. Smartphone-based NIR fluorescent imaging is still an emerging technology, but the performance of the built-in camera has been confirmed to be effective in capturing NIR fluorescent images. Based on the source and the development trend of this technology, we demonstrated that smartphone-based non-invasive bacteria/virus/cell detection should be the shape of things to come. Therefore, in this review, several issues were discussed including the incorporation of microfabrication techniques, the development of brighter/species-specific/wash-free NIR fluorophores, and smartphone-based telemedicine (Table 4). All in all, based on the considerable progress in the development of NIR fluorophores, mobile phones, and other peripheral technologies, a smartphone-based microscope system should be a key technology that connects the functionality of NIR fluorescent imaging with POC.

Author contributions

Wenjing HUANG did most writing and literature review of the manuscript. Shenglin LUO contributed partial writing and some literature review. Dong YANG edited the manuscript. Sheng ZHANG contributed the framework of the manuscript and supervised the process. All authors have read and approved the final manuscript and, therefore, have full access to all the data in the study and take responsibility for the integrity and security of the data.

Table 4 Related techniques promoting smartphone-based NIR fluorescent imaging

Technique	Effectiveness	Reference
Grating for smartphone	1. Spectral coverage from the visible to near-infrared spectral regions; 2. High wavelength resolution; 3. Low cost	Pügner et al., 2016; McGonigle et al., 2018
Three-dimensional (3D) printing techniques	1. Low-cost fabrication for device housings; 2. Customizable design of optics equipment	Zhang et al., 2013; Arafat Hossain et al., 2015; Wilkes et al., 2017
Bacteria-specific probes	Detection of specific bacteria harmful to human beings	Stoye and Coffin, 1988; Chou et al., 2006
Smartphone-based cell separation/sorting	Basic diagnostic processes	Koydemir et al., 2015; Knowlton et al., 2017
Smartphone-based telemedicine	Synergistic effects	McCartney, 2014; Cunningham and Bolley, 2016

Compliance with ethics guidelines

Wenjing HUANG, Shenglin LUO, Dong YANG, and Sheng ZHANG declare that they have no conflict of interest.

All procedures followed were in accordance with the ethical standards of the responsible committee on human experimentation (institutional and national) and with the Helsinki Declaration of 1975, as revised in 2008 (5). Informed consent was obtained from all patients for being included in the study. Additional informed consent was obtained from all patients for whom identifying information is included in this article.

References

Achigui HF, Sawan M, Fayomi CJB, 2008. A monolithic based NIRS front-end wireless sensor. *Microelectronics J*, 39(10): 1209-1217.
https://doi.org/10.1016/j.mejo.2008.01.055

Antaris AL, Chen H, Cheng K, et al., 2016. A small-molecule dye for NIR-II imaging. *Nat Mater*, 15(2):235-242.
https://doi.org/10.1038/nmat4476

Arafat Hossain M, Canning J, Ast S, et al., 2015. Combined "dual" absorption and fluorescence smartphone spectrometers. *Opt Lett*, 40(8):1737-1740.
https://doi.org/10.1364/ol.40.001737

Baldursson S, Karanis P, 2011. Waterborne transmission of protozoan parasites: review of worldwide outbreaks—an update 2004–2010. *Water Res*, 45(20):6603-6614.
https://doi.org/10.1016/j.watres.2011.10.013

Berlec A, Štrukelj B, 2014. A high-throughput biliverdin assay using infrared fluorescence. *J Vet Diagn Invest*, 26(4):521-526.
https://doi.org/10.1177/1040638714535403

Berlec A, Završnik J, Butinar M, et al., 2015. *In vivo* imaging of *Lactococcus lactis*, *Lactobacillus plantarum* and *Escherichia coli* expressing infrared fluorescent protein in mice. *Microb Cell Fact*, 14:181.
https://doi.org/10.1186/s12934-015-0376-4

Breslauer DN, Maamari RN, Switz NA, et al., 2009. Mobile phone based clinical microscopy for global health applications. *PLoS ONE*, 4(7):e6320.
https://doi.org/10.1371/journal.pone.0006320

Bui N, Nguyen A, Nguyen P, et al., 2017. PhO₂: smartphone based blood oxygen level measurement systems using near-IR and RED wave-guided light. Proceedings of the 15th ACM Conference on Embedded Network Sensor Systems CD-ROM. ACM, New York, USA, p.230-244.
https://doi.org/10.1145/3131672.3131696

Ceylan Koydemir H, Ozcan A, 2018. Smartphones democratize advanced biomedical instruments and foster innovation. *Clin Pharmacol Ther*, 104(1):38-41.
https://doi.org/10.1002/cpt.1081

Chance B, Nioka S, Kent J, et al., 1988. Time-resolved spectroscopy of hemoglobin and myoglobin in resting and ischemic muscle. *Anal Biochem*, 174(2):698-707.
https://doi.org/10.1016/0003-2697(88)90076-0

Chen CY, Hofherr SE, Schwegel JS, et al., 2008. Real-time near infrared fluorescence imaging of viruses and ligands. *Mol Ther*, 16(S1):S21.
https://doi.org/10.1016/S1525-0016(16)39455-2

Chen ZY, Zhu N, Pacheco S, et al., 2014. Single camera imaging system for color and near-infrared fluorescence image guided surgery. *Biomed Opt Express*, 5(8):2791-2797.
https://doi.org/10.1364/BOE.5.002791

Chou CC, Lee TT, Chen CH, et al., 2006. Design of microarray probes for virus identification and detection of emerging viruses at the genus level. *BMC Bioinformatics*, 7:232.
https://doi.org/10.1186/1471-2105-7-232

Chung S, Breshears LE, Yoon JY, 2018. Smartphone near infrared monitoring of plant stress. *Comput Electron Agric*, 154:93-98.
https://doi.org/10.1016/j.compag.2018.08.046

Cunningham BP, Bolley B, 2016. Telemedicine and smartphones: is there a role for technology in the austere environment? *In*: de Dios Robinson J (Ed.), Orthopaedic Trauma in the Austere Environment: A Practical Guide to Care in the Humanitarian Setting. Springer, Cham, p.677-683.
https://doi.org/10.1007/978-3-319-29122-2_51

Dias DDS, 2015. Design of a Low-Cost Wireless NIRS System with Embedded Linux and a Smartphone Interface. MS Thesis, Wright State University, Ohio, USA.

Ding D, Li K, Liu B, et al., 2013. Bioprobes based on AIE fluorogens. *Acc Chem Res*, 46(11):2441-2453.
https://doi.org/10.1021/ar3003464

Dinjaski N, Suri S, Valle J, et al., 2014. Near-infrared fluorescence imaging as an alternative to bioluminescent bacteria to monitor biomaterial-associated infections. *Acta Biomater*, 10(7):2935-2944.
https://doi.org/10.1016/j.actbio.2014.03.005

Foster AE, Kwon S, Ke S, et al., 2008. *In vivo* fluorescent optical imaging of cytotoxic T lymphocyte migration using IRDye800CW near-infrared dye. *Appl Opt*, 47(31): 5944-5952.
https://doi.org/10.1364/AO.47.005944

Frangioni JV, 2003. *In vivo* near-infrared fluorescence imaging. *Curr Opin Chem Biol*, 7(5):626-634.
https://doi.org/10.1016/j.cbpa.2003.08.007

Fu MY, Xiao Y, Qian XH, et al., 2008. A design concept of long-wavelength fluorescent analogs of rhodamine dyes: replacement of oxygen with silicon atom. *Chem Commun*, (15):1780-1782.
https://doi.org/10.1039/b718544h

Ghassemi P, Wang BH, Wang JT, et al., 2017. Evaluation of mobile phone performance for near-infrared fluorescence imaging. *IEEE Trans Biomed Eng*, 64(7):1650-1653.
https://doi.org/10.1109/tbme.2016.2601014

Gopinath SCB, Tang TH, Chen Y, et al., 2014. Bacterial detection: from microscope to smartphone. *Biosens Bioelectron*, 60: 332-342.
https://doi.org/10.1016/j.bios.2014.04.014

Handa T, Katare RG, Sasaguri S, et al., 2009. Preliminary experience for the evaluation of the intraoperative graft patency with real color charge-coupled device camera system: an advanced device for simultaneous capturing of color and near-infrared images during coronary artery bypass graft. *Interact Cardiovasc Thorac Surg*, 9(2):150-154.
https://doi.org/10.1510/icvts.2008.201418

Haspot F, Lavault A, Sinzger C, et al., 2012. Human cytomegalovirus entry into dendritic cells occurs via a macropinocytosis-like pathway in a pH-independent and cholesterol-dependent manner. *PLoS ONE*, 7(4):e34795.
https://doi.org/10.1371/journal.pone.0034795

Heuker M, Gomes A, van Dijl JM, et al., 2016. Preclinical studies and prospective clinical applications for bacteria-targeted imaging: the future is bright. *Clin Transl Imaging*, 4(4):253-264.
https://doi.org/10.1007/s40336-016-0190-y

Hol FJH, Dekker C, 2014. Zooming in to see the bigger picture: microfluidic and nanofabrication tools to study bacteria. *Science*, 346(6208):1251821.
https://doi.org/10.1126/science.1251821

Holz C, Ofek E, 2018. Doubling the signal quality of smartphone camera pulse oximetry using the display screen as a controllable selective light source. Proceedings of the 40th Annual International Conference of the IEEE Engineering in Medicine and Biology Society, p.1-4.
https://doi.org/10.1109/EMBC.2018.8513286

Hong GS, Antaris AL, Dai HJ, 2017. Near-infrared fluorophores for biomedical imaging. *Nat Biomed Eng*, 1:0010.
https://doi.org/10.1038/s41551-016-0010

Huang ES, Johnson RA, 2000. Human cytomegalovirus—no longer just a DNA virus. *Nat Med*, 6(8):863.
https://doi.org/10.1038/78612

Hussain I, Bora AJ, Sarma D, et al., 2018. Design of a smartphone platform compact optical system operational both in visible and near infrared spectral regime. *IEEE Sens J*, 18(12):4933-4939.
https://doi.org/10.1109/jsen.2018.2832848

Hyun H, Wada H, Bao K, et al., 2014. Phosphonated near-infrared fluorophores for biomedical imaging of bone. *Angew Chem Int Ed*, 53(40):10668-10672.
https://doi.org/10.1002/anie.201404930

Hyun H, Owens EA, Wada H, et al., 2015. Cartilage-specific near-infrared fluorophores for biomedical imaging. *Angew Chem Int Ed*, 54(30):8648-8652.
https://doi.org/10.1002/anie.201502287

Isomura M, Yamada K, Noguchi K, et al., 2017. Near-infrared fluorescent protein iRFP720 is optimal for *in vivo* fluorescence imaging of rabies virus infection. *J Gen Virol*, 98(11):2689-2698.
https://doi.org/10.1099/jgv.0.000950

Kaile K, Godavarty A, 2019. Development and validation of a smartphone-based near-infrared optical imaging device to measure physiological changes in-vivo. *Micromachines*, 10(3):180.

https://doi.org/10.3390/mi10030180

Kanva AK, Sharma CJ, Deb S, 2014. Determination of SpO$_2$ and heart-rate using smartphone camera. Proceedings of International Conference on Control, Instrumentation, Energy and Communication, p.237-241.
https://doi.org/10.1109/CIEC.2014.6959086

Kim CK, Lee S, Koh D, et al., 2011. Development of wireless NIRS system with dynamic removal of motion artifacts. *Biomed Eng Lett*, 1(4):254-259.
https://doi.org/10.1007/s13534-011-0042-7

Kim JG, Liu H, 2007. Variation of haemoglobin extinction coefficients can cause errors in the determination of haemoglobin concentration measured by near-infrared spectroscopy. *Phys Med Biol*, 52(20):6295-6322.
https://doi.org/10.1088/0031-9155/52/20/014

Kleerebezem M, Beerthuyzen MM, Vaughan EE, et al., 1997. Controlled gene expression systems for lactic acid bacteria: transferable nisin-inducible expression cassettes for *Lactococcus*, *Leuconostoc*, and *Lactobacillus* spp. *Appl Environ Microbiol*, 63(11):4581-4584.
https://doi.org/10.1128/AEM.63.11.4581-4584.1997

Knowlton S, Joshi A, Syrrist P, et al., 2017. 3D-printed smartphone-based point of care tool for fluorescence- and magnetophoresis-based cytometry. *Lab Chip*, 17(16): 2839-2851.
https://doi.org/10.1039/c7lc00706j

Koide Y, Urano Y, Hanaoka K, et al., 2011. Evolution of group 14 rhodamines as platforms for near-infrared fluorescence probes utilizing photoinduced electron transfer. *ACS Chem Biol*, 6(6):600-608.
https://doi.org/10.1021/cb1002416

Koydemir HC, Gorocs Z, Tseng D, et al., 2015. Rapid imaging, detection and quantification of *Giardia lamblia* cysts using mobile-phone based fluorescent microscopy and machine learning. *Lab Chip*, 15(5):1284-1293.
https://doi.org/10.1039/c4lc01358a

Kühnemund M, Wei QS, Darai E, et al., 2017. Targeted DNA sequencing and *in situ* mutation analysis using mobile phone microscopy. *Nat Commun*, 8:13913.
https://doi.org/10.1038/ncomms13913

Liang PS, Park TS, Yoon JY, 2014. Rapid and reagentless detection of microbial contamination within meat utilizing a smartphone-based biosensor. *Sci Rep*, 4:5953.
https://doi.org/10.1038/srep05953

Long KD, Woodburn EV, Le HM, et al., 2017. Multimode smartphone biosensing: the transmission, reflection, and intensity spectral (TRI)-analyzer. *Lab Chip*, 17(19):3246-3257.
https://doi.org/10.1039/c7lc00633k

Lukinavičius G, Umezawa K, Olivier N, et al., 2013. A near-infrared fluorophore for live-cell super-resolution microscopy of cellular proteins. *Nat Chem*, 5(2):132-139.
https://doi.org/10.1038/nchem.1546

Luo JD, Xie ZL, Lam JWY, et al., 2001. Aggregation-induced emission of 1-methyl-1,2,3,4,5-pentaphenylsilole. *Chem*

Commun, 36(18):1740-1741.
https://doi.org/10.1039/b105159h

Luo SL, Zhang EL, Su YP, et al., 2011. A review of NIR dyes in cancer targeting and imaging. *Biomaterials*, 32(29):7127-7138.
https://doi.org/10.1016/j.biomaterials.2011.06.024

Männik J, Wu FB, Hol FJH, et al., 2012. Robustness and accuracy of cell division in *Escherichia coli* in diverse cell shapes. *Proc Natl Acad Sci USA*, 109(18):6957-6962.
https://doi.org/10.1073/pnas.1120854109

Marshall MV, Rasmussen JC, Tan IC, et al., 2010. Near-infrared fluorescence imaging in humans with indocyanine green: a review and update. *Open Surg Oncol J*, 2(2):12-25.
https://doi.org/10.2174/1876504101002010012

McAuliffe KJ, Kaster MA, Szlag RG, et al., 2017. Low-symmetry mixed fluorinated subphthalocyanines as fluorescence imaging probes in MDA-MB-231 breast tumor cells. *Int J Mol Sci*, 18(6):1177.
https://doi.org/10.3390/ijms18061177

McCartney P, 2014. Smart phones transform patient-centered telemedicine. *MCN*, 39(6):382.
https://doi.org/10.1097/nmc.0000000000000087

McGonigle AJS, Wilkes TC, Pering TD, et al., 2018. Smart-phone spectrometers. *Sensors (Basel)*, 18(1):223.
https://doi.org/10.3390/s18010223

Mei J, Leung NLC, Kwok RTK, et al., 2015. Aggregation-induced emission: together we shine, united we soar! *Chem Rev*, 115(21):11718-11940.
https://doi.org/10.1021/acs.chemrev.5b00263

Michael B, 2010. Optical Properties of Films and Coatings Handbook of Optics: Volume IV-Optical Properties of Materials, Nonlinear Optics, Quantum Optics, 3rd Ed. McGraw Hill Professional, Access Engineering.

Mierau I, Kleerebezem M, 2005. 10 years of the nisin-controlled gene expression system (NICE) in *Lactococcus lactis*. *Appl Microbiol Biotechnol*, 68(6):705-717.
https://doi.org/10.1007/s00253-005-0107-6

Mirica KA, Shevkoplyas SS, Phillips ST, et al., 2009. Measuring densities of solids and liquids using magnetic levitation: fundamentals. *J Am Chem Soc*, 131(29):10049-10058.
https://doi.org/10.1021/ja900920s

Nemiroski A, Kumar AA, Soh S, et al., 2016. High-sensitivity measurement of density by magnetic levitation. *Anal Chem*, 88(5):2666-2674.
https://doi.org/10.1021/acs.analchem.5b03918

Neuman BP, Eifler JB, Castanares M, et al., 2015. Real-time, near-infrared fluorescence imaging with an optimized dye/light source/camera combination for surgical guidance of prostate cancer. *Clin Cancer Res*, 21(4):771-780.
https://doi.org/10.1158/1078-0432.ccr-14-0891

Owens EA, Henary M, el Fakhri G, et al., 2016. Tissue-specific near-infrared fluorescence imaging. *Acc Chem Res*, 49(9):1731-1740.
https://doi.org/10.1021/acs.accounts.6b00239

Pan H, Zhang PF, Gao DY, et al., 2014. Noninvasive visual-ization of respiratory viral infection using bioorthogonal conjugated near-infrared-emitting quantum dots. *ACS Nano*, 8(6):5468-5477.
https://doi.org/10.1021/nn501028b

Pansare VJ, Hejazi S, Faenza WJ, et al., 2012. Review of long-wavelength optical and NIR imaging materials: contrast agents, fluorophores, and multifunctional nano carriers. *Chem Mater*, 24(5):812-827.
https://doi.org/10.1021/cm2028367

Pügner T, Knobbe J, Grüger H, 2016. Near-infrared grating spectrometer for mobile phone applications. *Appl Spectrosc*, 70(5):734-745.
https://doi.org/10.1177/0003702816638277

Qi P, Zhang D, Sun Y, et al., 2016. A selective near-infrared fluorescent probe for hydrogen sulfide and its application in sulfate-reducing bacteria detection. *Anal Methods*, 8(16):3339-3344.
https://doi.org/10.1039/c6ay00054a

Rateni G, Dario P, Cavallo F, 2017. Smartphone-based food diagnostic technologies: a review. *Sensors (Basel)*, 17(6):1453.
https://doi.org/10.3390/s17061453

Rolfe P, 2000. *In vivo* near-infrared spectroscopy. *Annu Rev Biomed Eng*, 2:715-754.
https://doi.org/10.1146/annurev.bioeng.2.1.715

Safaie J, Grebe R, Moghaddam HA, et al., 2013. Wireless distrib-uted acquisition system for near infrared spectroscopy—WDA-NIRS. *J Innov Opt Health Sci*, 6(3):1350019.
https://doi.org/10.1142/s1793545813500193

Sakuda T, Kubo T, Johan MP, et al., 2019. Novel near-infrared fluorescence-guided surgery with vesicular stomatitis virus for complete surgical resection of osteosarcomas in mice. *J Orthop Res*, 37(5):1192-1201.
https://doi.org/10.1002/jor.24277

Schaafsma BE, Mieog JSD, Hutteman M, et al., 2011. The clinical use of indocyanine green as a near-infrared fluorescent contrast agent for image-guided oncologic surgery. *J Surg Oncol*, 104(3):323-332.
https://doi.org/10.1002/jso.21943

Scott AS, Baltzan MA, Wolkove N, 2014. Examination of pulse oximetry tracings to detect obstructive sleep apnea in patients with advanced chronic obstructive pulmonary disease. *Can Respir J*, 21:948717.
https://doi.org/10.1155/2014/948717

Sevick-Muraca EM, Sharma R, Rasmussen JC, et al., 2008. Imaging of lymph flow in breast cancer patients after microdose administration of a near-infrared fluorophore: feasibility study. *Radiology*, 246(3):734-741.
https://doi.org/10.1148/radiol.2463070962

Shcherbakova DM, Baloban M, Emelyanov AV, et al., 2016. Bright monomeric near-infrared fluorescent proteins as tags and biosensors for multiscale imaging. *Nat Commun*, 7:12405.

https://doi.org/10.1038/ncomms12405

Shcherbo D, Shemiakina II, Ryabova AV, et al., 2010. Near-infrared fluorescent proteins. *Nat Methods*, 7(10):827-829.
https://doi.org/10.1038/nmeth.1501

Shieh P, Siegrist MS, Cullen AJ, et al., 2014. Imaging bacterial peptidoglycan with near-infrared fluorogenic azide probes. *Proc Natl Acad Sci USA*, 111(15):5456-5461.
https://doi.org/10.1073/pnas.1322727111

Shu XK, Royant A, Lin MZ, et al., 2009. Mammalian expression of infrared fluorescent proteins engineered from a bacterial phytochrome. *Science*, 324(5928):804-807.
https://doi.org/10.1126/science.1168683

Sletten EM, Bertozzi CR, 2009. Bioorthogonal chemistry: fishing for selectivity in a sea of functionality. *Angew Chem Int Ed*, 48(38):6974-6998.
https://doi.org/10.1002/anie.200900942

Smith ZJ, Chu KQ, Espenson AR, et al., 2011. Cell-phone-based platform for biomedical device development and education applications. *PLoS ONE*, 6(3):e17150.
https://doi.org/10.1371/journal.pone.0017150

Stoye JP, Coffin JM, 1988. Polymorphism of murine endogenous proviruses revealed by using virus class-specific oligonu-cleotide probes. *J Virol*, 62(1):168-175.
https://doi.org/10.1128/JVI.62.1.168-175.1988

Strangman G, Franceschini MA, Boas DA, 2003. Factors affecting the accuracy of near-infrared spectroscopy concentration calculations for focal changes in oxygenation parameters. *NeuroImage*, 18(4):865-879.
https://doi.org/10.1016/S1053-8119(03)00021-1

Suresh N, Tang QG, Liu Y, et al., 2018. Characterization and *in vivo* application of mobile phones for near-infrared fluorescence imaging of tumors. Proceedings of Frontiers in Optics 2018, Washington DC, USA.
https://doi.org/10.1364/FIO.2018.JW3A.117

Tan X, Luo SL, Long L, et al., 2017. Structure-guided design and synthesis of a mitochondria-targeting near-infrared fluorophore with multimodal therapeutic activities. *Adv Mater*, 29(43):1704196.
https://doi.org/10.1002/adma.201704196

Tang R, Xue JP, Xu BG, et al., 2015. Tunable ultrasmall visible-to-extended near-infrared emitting silver sulfide quantum dots for integrin-targeted cancer imaging. *ACS Nano*, 9(1):220-230.
https://doi.org/10.1021/nn5071183

Troyan SL, Kianzad V, Gibbs-Strauss SL, et al., 2009. The FLARE™ intraoperative near-infrared fluorescence imaging system: a first-in-human clinical trial in breast cancer sentinel lymph node mapping. *Ann Surg Oncol*, 16(10):2943-2952.
https://doi.org/10.1245/s10434-009-0594-2

Urano Y, Asanuma D, Hama Y, et al., 2008. Selective molecular imaging of viable cancer cells with pH-activatable fluo-rescence probes. *Nat Med*, 15:104-109.
https://doi.org/10.1038/nm.1854

Vaithianathan T, Tullis IDC, Everdell N, et al., 2004. Design of a portable near infrared system for topographic imaging of the brain in babies. *Rev Sci Instrum*, 75(10):3276-3283.
https://doi.org/10.1063/1.1775314

Vanegas M, Carp S, Fang QQ, 2018. Mobile phone camera based near-infrared spectroscopy measurements. Proceedings of Clinical and Translational Biophotonics 2018, Hollywood, Florida, USA.
https://doi.org/10.1364/TRANSLATIONAL.2018.JTu3A.64

Ventola CL, 2014. Mobile devices and apps for health care professionals: uses and benefits. *P T*, 39(5):356-364.

Wang P, Robert L, Pelletier J, et al., 2010. Robust growth of *Escherichia coli*. *Curr Biol*, 20(12):1099-1103.
https://doi.org/10.1016/j.cub.2010.04.045

Watanabe T, Sekine R, Mizuno T, et al., 2016. Development of portable, wireless and smartphone controllable near-infrared spectroscopy system. *In*: Luo QM, Li LZ, Harrison DK, et al. (Eds.), Oxygen Transport to Tissue XXXVIII. Springer, Cham, p.385-392.
https://doi.org/10.1007/978-3-319-38810-6_50

Wei QS, Qi HF, Luo W, et al., 2013. Fluorescent imaging of single nanoparticles and viruses on a smart phone. *ACS Nano*, 7(10):9147-9155.
https://doi.org/10.1021/nn4037706

Wei QS, Luo W, Chiang S, et al., 2014. Imaging and sizing of single DNA molecules on a mobile phone. *ACS Nano*, 8(12):12725-12733.
https://doi.org/10.1021/nn505821y

Wilkes TC, McGonigle AJS, Willmott JR, et al., 2017. Low-cost 3D printed 1 nm resolution smartphone sensor-based spectrometer: instrument design and application in ultraviolet spectroscopy. *Opt Lett*, 42(21):4323-4326.
https://doi.org/10.1364/ol.42.004323

Wu FB, van Rijn E, van Schie BGC, et al., 2015a. Multi-color imaging of the bacterial nucleoid and division proteins with blue, orange, and near-infrared fluorescent proteins. *Front Microbiol*, 6:607.
https://doi.org/10.3389/fmicb.2015.00607

Wu FB, van Schie BGC, Keymer JE, et al., 2015b. Symmetry and scale orient Min protein patterns in shaped bacterial sculptures. *Nat Nanotechnol*, 10(8):719-726.
https://doi.org/10.1038/nnano.2015.126

Yoo JH, 2013. The meaning of information technology (IT) mobile devices to me, the infectious disease physician. *Infect Chemother*, 45(2):244-251.
https://doi.org/10.3947/ic.2013.45.2.244

Zhang CL, Anzalone NC, Faria RP, et al., 2013. Open-source 3D-printable optics equipment. *PLoS ONE*, 8(3):e59840.
https://doi.org/10.1371/journal.pone.0059840

Zhang Y, Sun JW, Wei G, et al., 2009. Design of a portable near infra-red spectroscopy system for tissue oxygenation measurement. Proceedings of the 3rd International Con-ference on Bioinformatics and Biomedical Engineering,

Beijing, China.
https://doi.org/10.1109/ICBBE.2009.5162593

Zhao EG, Chen YL, Wang H, et al., 2015a. Light-enhanced bacterial killing and wash-free imaging based on AIE fluorogen. *ACS Appl Mater Interfaces*, 7(13):7180-7188.
https://doi.org/10.1021/am509142k

Zhao EG, Chen YL, Chen SJ, et al., 2015b. A luminogen with aggregation-induced emission characteristics for wash-free bacterial imaging, high-throughput antibiotics screening and bacterial susceptibility evaluation. *Adv Mater*, 27(33):4931-4937.
https://doi.org/10.1002/adma.201501972

Zhao JY, Zhong D, Zhou SB, 2018. NIR-I-to-NIR-II fluorescent nanomaterials for biomedical imaging and cancer therapy. *J Mater Chem B*, 6(3):349-365.
https://doi.org/10.1039/c7tb02573d

Zhou J, Yang F, Jiang GC, et al., 2016. Applications of indocyanine green based near-infrared fluorescence imaging in thoracic surgery. *J Thorac Dis*, 8(S9):S738-S743.
https://doi.org/10.21037/jtd.2016.09.49

Zhou XX, Li WF, Ma GX, et al., 2006. The nisin-controlled gene expression system: construction, application and improvements. *Biotechnol Adv*, 24(3):285-295.
https://doi.org/10.1016/j.biotechadv.2005.11.001

Zhu B, Sevick-Muraca EM, 2015. A review of performance of near-infrared fluorescence imaging devices used in clinical studies. *Br J Radiol*, 88(1045):20140547.
https://doi.org/10.1259/bjr.20140547

Zhu BH, Rasmussen JC, Lu YJ, et al., 2010. Reduction of excitation light leakage to improve near-infrared fluorescence imaging for tissue surface and deep tissue imaging. *Med Phys*, 37(11):5961-5970.
https://doi.org/10.1118/1.3497153

Zhu HY, Yaglidere O, Su TW, et al., 2011a. Cost-effective and compact wide-field fluorescent imaging on a cell-phone. *Lab Chip*, 11(2):315-322.
https://doi.org/10.1039/c0lc00358a

Zhu HY, Mavandadi S, Coskun AF, et al., 2011b. Optofluidic fluorescent imaging cytometry on a cell phone. *Analy Chem*, 83(17):6641-6647.
https://doi.org/10.1021/ac201587a

Zhu HY, Yaglidere O, Su TW, et al., 2011c. Wide-field fluorescent microscopy on a cell-phone. Proceedings of Annual International Conference of the IEEE Engineering in Medicine and Biology Society, Boston, MA, USA.
https://doi.org/10.1109/IEMBS.2011.6091677

Zhu HY, Sikora U, Ozcan A, 2012. Quantum dot enabled detection of *Escherichia coli* using a cell-phone. *Analyst*, 137(11):2541-2544.
https://doi.org/10.1039/c2an35071h